

Cardiac acetylcholine inhibits ventricular remodeling and dysfunction under pathologic conditions

Ashbeel Roy,^{*,†} Mouhamed Dakroub,^{*,†} Geisa C. S. V. Tezini,[¶] Yin Liu,[†] Silvia Guatimosim,^{||} Qingping Feng,^{†,‡} Helio C. Salgado,[¶] Vania F. Prado,^{*,†,§} Marco A. M. Prado,^{*,†,§,1} and Robert Gros^{*,†,‡,1}

^{*}Robarts Research Institute, [†]Department of Physiology and Pharmacology, [‡]Department of Medicine, and [§]Department of Anatomy and Cell Biology, The University of Western Ontario, London, Ontario, Canada; [¶]Department of Physiology, School of Medicine of Ribeirão Preto, University of São Paulo, Ribeirão Preto, Brazil; and ^{||}Department of Physiology and Biophysics, Institute of Biological Sciences, Federal University of Minas Gerais, Belo Horizonte, Brazil

ABSTRACT Autonomic dysfunction is a characteristic of cardiac disease and decreased vagal activity is observed in heart failure. Rodent cardiomyocytes produce *de novo* ACh, which is critical in maintaining cardiac homeostasis. We report that this nonneuronal cholinergic system is also found in human cardiomyocytes, which expressed choline acetyltransferase (ChAT) and the vesicular acetylcholine transporter (VAcHT). Furthermore, VAcHT expression was increased 3- and 1.5-fold at the mRNA and protein level, respectively, in ventricular tissue from patients with heart failure, suggesting increased ACh secretion in disease. We used mice with genetic deletion of cardiomyocyte-specific VAcHT or ChAT and mice overexpressing VAcHT to test the functional significance of cholinergic signaling. Mice deficient for VAcHT displayed an 8% decrease in fractional shortening and 13% decrease in ejection fraction compared with angiotensin II (Ang II)-treated control animals, suggesting enhanced ventricular dysfunction and pathologic remodeling in response to Ang II. Similar results were observed in ChAT-deficient mice. Conversely, no decline in ventricular function was observed in Ang II-treated VAcHT overexpressors. Furthermore, the fibrotic area was significantly greater ($P < 0.05$) in Ang II-treated VAcHT-deficient mice ($3.61 \pm 0.64\%$) compared with wild-type animals ($2.24 \pm 0.11\%$). In contrast, VAcHT overexpressing mice did not display an increase in collagen deposition. Our results provide new insight into cholinergic regulation of cardiac function, suggesting that a compensatory increase in cardiomyocyte VAcHT levels may help offset cardiac remodeling in heart failure.—Roy, A., Dakroub, M., Tezini, G. C. S. V., Liu, Y., Guatimosim, S., Feng, Q., Salgado, H. C., Prado, V. F., Prado, M. A. M., Gros, R. Cardiac acetylcholine inhibits ventricular remodeling and dysfunction under pathologic conditions. *FASEB J.* 30, 688–701 (2016). www.fasebj.org

Key Words: heart disease • choline acetyltransferase • heart failure • nonneuronal acetylcholine • VAcHT

It is well established that chronic autonomic sympathetic/parasympathetic imbalance plays a crucial role in the development of heart failure (HF) (1–4). There appears to be a significant increase in adrenergic signaling in HF, even in the initial stages of cardiac remodeling before the onset of heart dysfunction (5). The hyperadrenergic state contributes to cardiac remodeling (5, 6), and this correlates with higher morbidity and mortality (7).

Early changes in autonomic control in HF also involve decreased parasympathetic regulation (8–10). Altered heart rate (HR) regulation due to changes in vagal nerve activity has been observed shortly after induction of left ventricular (LV) dysfunction (11). However, how compensatory changes in cholinergic signaling could contribute to development of HF is still not fully understood.

Previous experiments have suggested that compensatory transdifferentiation of sympathetic neurons to a cholinergic phenotype during HF can help offset mortality, suggesting a protective role for this compensatory mechanism (12). In an animal model of HF, concomitant treatment using vagal nerve stimulation and β -blockade therapy has been shown to improve cardiac contractility and animal survival (13, 14). Furthermore, both cardiac remodeling and mortality were reduced in animal models of HF after chronic treatment with the cholinesterase inhibitor donepezil (15, 16). Finally, increasing extracellular ACh levels through administration of a peripheral quaternary cholinesterase inhibitor, pyridostigmine, led to greater vagal control of the heart and reduced ventricular dysfunction in rats with HF (17, 18).

A clinical trial investigating vagal stimulation *via* an implantable system indicates that treated patients presented

Abbreviations: ACh, acetylcholine; AChE, acetylcholinesterase; Ang II, angiotensin II; BAC, bacterial artificial chromosome; cChAT, cardiomyocyte-specific ChAT knockout; ChAT, choline acetyltransferase; ChR2, channelrhodopsin-2; cVAcHT, cardiomyocyte-specific VAcHT knockout; Floxed, flanked by loxP; HF, heart failure; HR, heart rate; KO,

(continued on next page)

¹ Correspondence: Robarts Research Institute, 1151 Richmond St. N, The University of Western Ontario, London, ON, Canada N6A 5B7. E-mail: mprado@robarts.ca (M.A.M.P.); rgros@robarts.ca (R.G.)

doi: 10.1096/fj.15-277046

This article includes supplemental data. Please visit <http://www.fasebj.org> to obtain this information.

an improvement in New York Heart Association class score as well as LV end-systolic volume, which refers to the residual blood in the heart after contraction (19). Moreover, epidemiologic observation revealed that patients with Alzheimer disease receiving cholinesterase inhibitors present decreased risk of myocardial infarction and cardiovascular death compared with patients who did not receive or who received lower doses of cholinesterase inhibitors (20).

Distinct ways to genetically disturb cholinergic activity in mice suggest that intact cholinergic signaling is critical for heart health and ventricular function (21–24), despite the sparse levels of cholinergic innervation outside the atria (25). Regulated autocrine/paracrine secretion of non-neuronal ACh by cardiomyocytes has recently emerged as a new mechanism by which heart cells can regulate and increase parasympathetic signaling (26). In support of this mechanism, cardiomyocyte overexpression of choline acetyltransferase (ChAT) and ACh in transgenic mice protects against myocardial infarction (24). In addition, cardiomyocyte-selective elimination of the vesicular acetylcholine transporter (VAcHT), a protein responsible for packing ACh in secretory vesicles, led to altered cardiovascular regulation during exercise and induced early-stage cardiac remodeling and cardiomyocyte stress (21).

Here we found that both healthy and diseased human cardiomyocytes express *bona fide* presynaptic markers of the cholinergic system, namely ChAT and VAcHT. Furthermore, LV tissue from human patients with nonischemic dilated cardiomyopathy (NICM) displayed a significant increase in the expression of VAcHT, including VAcHT present in cardiomyocytes, compared with age-matched controls.

In order to further examine the importance of the non-neuronal cholinergic system (NNCS) in cardiac disease, we used genetically modified mice in which either VAcHT or ChAT was selectively deleted from cardiomyocytes or in which VAcHT was overexpressed. The mice were chronically treated with angiotensin II (Ang II) to induce limited cardiac remodeling resulting from chronic vasoconstriction as well as direct effects of Ang II on ventricular cardiomyocytes. This approach allowed us to determine the role of the cholinergic system in the early stages of cardiac disease, before the onset of HF. Our animal data suggest that compensatory changes in VAcHT levels in humans may play a role in mitigating the extent of cardiac remodeling in HF.

MATERIALS AND METHODS

Human tissue samples

LV tissue samples were obtained from the Duke Human Heart Repository (Durham, NC, USA). LV myocardium was obtained from 7 HF patients with NICM and age-matched nonfailing individuals. LV tissue was flash frozen for RNA and protein extraction and embedded in optimal cutting temperature compound for

(continued from previous page)

knockout; LV, left ventricular; LVID, left ventricular internal systolic dimension; LVIDd, left ventricular internal end-diastolic dimension; NICM, nonischemic dilated cardiomyopathy; NNCS, non-neuronal cholinergic system; qPCR, quantitative polymerase chain reaction; RT-PCR, reverse transcription-polymerase chain reaction; VAcHT, vesicular acetylcholine transporter; WT, wild type

immunostaining. The use of these samples was approved by the institutional review board at Duke University Medical Center (Durham, NC, USA).

Animal models

Only male mice aged 3 to 6 mo were used for all *in vivo* experiments. Cardiomyocyte-specific VAcHT- or ChAT-knockout (KO) [cVAcHT (VAcHT^{Myh6-Cre-VAcHT-flox/flox}) or cChAT (ChAT^{Myh6-Cre-ChAT-flox/flox})] mice were generated as described in a previous study (21). cVAcHT mice were back-crossed to the C57BL/6J background for at least 6 generations, and cChAT mice were back-crossed to the C57BL/6J background for at least 10 generations. Myh6-Cre+ (*B6.FVB-Tg(Myh6-cre)2182Mds/J*) mice were back-crossed to the C57BL/6J background for at least 10 generations. *ChAT-ChR2-EYFP* mice overexpressing the VAcHT (*B6.Cg-Tg(ChAT-COP4*H134R/EYFP,Slc18a3)6Gfng/J*) (27–29) were kindly donated by G. Feng (Massachusetts Institute of Technology, Boston, MA, USA) in 2012 and back-crossed to the C57BL/6J background for at least 6 generations (27, 29).

Ang II infusion to induce cardiac remodeling

Ang II (A9525; Sigma-Aldrich, St. Louis, MO, USA) was dissolved in sterile saline and added to osmotic pumps (model 1002; Alzet, New York, NY, USA) to deliver a dose of 3 mg/kg/d. The pumps were implanted subcutaneously, and Ang II or saline was infused for 2 wk. Mice were then housed for an additional 2 wk to allow remodeling before experimental use.

Echocardiography

M-mode echocardiography was performed after Ang II or saline treatments. LV and right ventricular ejection fraction and fractional shortening were measured with the Vevo 2100 ultrasound imaging system (VisualSonics, Toronto, ON, Canada). Briefly, 2-dimensional images of the heart were obtained in short-axis view using a dynamically focused 40 MHz probe. The M-mode cursor was positioned perpendicular to the LV anterior and posterior walls. The LV internal end-diastolic dimension (LVIDd) and LV internal systolic dimension (LVID) were measured from M-mode recordings. LV ejection fraction was calculated as: EF (%) = [(LVIDd)³ - (LVIDs)³] / (LVIDd)³ × 100. Fractional shortening was calculated as: FS (%) = (LVIDd - LVIDs) / LVIDd × 100. The M-mode measurements of the LV ejection fraction and fractional shortening were averaged from 3 cycles.

Reactive oxygen species measurement

Reactive oxygen species levels were measured using the MitoSOX Red superoxide indicator (Invitrogen, Carlsbad, CA, USA) as previously described (22).

Protein oxidation levels

Hearts from saline- or Ang II-treated mice were isolated, fixed, and embedded in paraffin. Tissue sections (5 μm) were obtained, and oxidized protein levels were analyzed using the OxyIHC Oxidative Stress Kit (EMD Millipore, Billerica, MA, USA) following the manufacturer's directions. Briefly, carbonyl groups on oxidized proteins are derivatized with 2,4-dinitrophenylhydrazine and the DNP-derivatized proteins detected using an antibody specific to the DNP moiety. This was followed by a standard immunohistochemistry procedure to stain oxidized proteins. The intensity of the staining was measured by ImageJ software (Image Processing and Analysis in Java; U.S. National Institutes of Health, Bethesda, MD, USA) to quantify the extent of protein oxidation.

Histologic analysis

Sections (5 μm) were obtained from saline- and Ang II-treated mice. The tissue sections were stained with hematoxylin and eosin using standard procedures. Light microscopic images were acquired at 20 \times magnification at distinct locations within the LV free wall.

Cardiomyocyte cell surface area was measured using hematoxylin and eosin-stained sections where cardiomyocyte edges were distinctly observable. Cell surface was measured in sections obtained from at least 4 mice per genotype.

Cardiac fibrosis

Sections (5 μm) obtained after Ang II or saline treatment were stained with Trichrome C using standard procedures to analyze extent of cardiac fibrosis. Light microscopic images were acquired at $\times 20$ magnification at separate locations within the LV wall to analyze both interstitial and perivascular collagen deposition.

Quantitative polymerase chain reaction/reverse transcription-polymerase chain reaction

Total RNA from flash frozen whole hearts or ventricular tissue was extracted using the Bio-Rad Aurum Total Fatty and Fibrous Tissue kit according to the manufacturer's protocol (Bio-Rad, Hercules, CA, USA). A total of 500 ng of total RNA was used to synthesize 20 μl of cDNA using the Applied Biosystems High Capacity cDNA Reverse Transcription Kit (Applied Biosystems, Foster City, CA, USA). The synthesized cDNA was diluted by half. The total reaction volume for quantitative polymerase chain reaction (qPCR) was as follows: 1 μl diluted cDNA, 2.5 μl SYBR Green, 0.5 μl each of the forward and reverse primers, and 0.5 μl of Milli-Q H_2O . Primers for VACHT, ChAT, acetylcholinesterase (AChE), β -myosin heavy chain, and atrial natriuretic peptide were designed to produce an amplicon of approximately 100 bp, and the specificity was determined using the National Center for Biotechnology Information Primer-Basic Local Alignment Search Tool. Specific primer sequences are provided in Supplemental Table S1. The qPCR reaction conditions were as follows: initial denaturation for 2 min at 94 $^\circ\text{C}$, followed by 40 cycles of denaturation (94 $^\circ\text{C}$, 15 s), annealing, and extension (60 $^\circ\text{C}$, 1 min). Relative expression of the gene of interest was analyzed using the $\Delta\Delta\text{C}_q$ calculation method. β -Actin and glyceraldehyde phosphate dehydrogenase (GAPDH) were used to normalize qPCR results for mice and humans, respectively. β -Actin was used as the reference gene to normalize the gene expression data for the animal studies because no variation in β -actin expression was observed across different genotypes or treatment groups. Similarly, no differences in GAPDH levels were observed in the human samples.

Immunoblotting

Protein was extracted from human and mouse LV tissue using ice-cold modified RIPA buffer. A total of 50 μg of protein was separated using SDS-PAGE and transferred to PVDF membranes, which were probed with anti-VACHT antibody (1:500; Synaptic Systems, Göttingen, Germany) or anti-ChAT antibody (1:500; Abcam, Cambridge, MA, USA). α -Actinin (1:2000; Sigma-Aldrich) was used as a loading control.

Immunostaining

Murine adult cardiomyocytes and atrial tissues were subjected to an immunostaining protocol as previously described (30). Cells

were costained with anti-ChAT (1:100; Abcam) and anti- α -actinin (1:200; Sigma-Aldrich) antibodies. α -Actinin-labeled cells were used to measure cardiomyocyte cell surface area. Atrial tissue was stained with anti-VACHT (1:200; Synaptic Systems). Hoechst 33342 (Life Technologies, Gibco, Carlsbad, CA, USA) was used as the nuclear marker. Images were acquired using the Zeiss LSM 510 Meta confocal system (Carl Zeiss GmbH, Jena, Germany).

For human LV tissue, 5 μm sections were subjected to the immunofluorescence protocol as previously described (30). The tissue was incubated with either anti-VACHT (1:100; Synaptic Systems) or anti-ChAT (1:100; Abcam) and anti- α -actinin (1:500; Sigma-Aldrich). Images were acquired using the $\times 63$ objective on the Zeiss LSM 510 Meta confocal system.

All imaging parameters, including laser power (Ar: 5%; HeNe₁ and HeNe₂: 10%) and pinhole size (1 airy unit), as well as PMT gain and offset, remained constant across all treatment groups imaged within a single experiment. The VACHT antibody utilized for these studies was previously validated in VACHT-KO mice and is known to specifically recognize VACHT in mammalian cardiomyocytes (21). The ChAT antibody does not recognize the protein in KO animals (Supplemental Fig. S1) and therefore is also specific.

Measurement of ACh secretion

Acetylcholine release was measured using the Choline/ACh Quantification Kit (BioVision, Milpitas, CA, USA) or HPLC with electrochemical detection as previously described (21, 31). Briefly, atrial tissue was isolated from wild-type (WT) and *ChAT-ChR2-EYFP* mice and incubated in Tyrode solution containing 100 μM pyridostigmine bromide (Sigma-Aldrich; P9797) at 37 $^\circ\text{C}$ for 2 h. The solution was collected and centrifuged at 10,000 rpm for 5 min at 4 $^\circ\text{C}$, and the resulting supernatant was collected and placed on ice. Each sample was assayed in duplicate, and experiments were conducted using at least 3 mice per genotype.

HR and blood pressure measurement

Systolic and diastolic blood pressure as well as HR were recorded from conscious animals using the CODA tail-cuff blood pressure system (Kent Scientific, Torrington, CT, USA) as previously described (21, 32).

Electrocardiography

Radiofrequency telemeters were implanted in WT and *ChAT-ChR2-EYFP* mice subcutaneously, and electrocardiogram recordings were obtained as previously described (21). HR was recorded continuously over 24 h to obtain baseline recordings. In addition, HR recordings were obtained immediately after intraperitoneal saline injection or after an acute exercise routine, as previously described (21).

Cardiac sympathovagal balance

After 60 min of basal HR recording, methylatropine (2 mg/kg, i.p.; Sigma-Aldrich) was injected, and the HR was recorded for the next 45 min to assess the effect of vagal blockade on the HR. Propranolol (5 mg/kg, i.p., Sigma-Aldrich) was then injected in the same mouse, and the HR was recorded for an additional 45 min to determine the intrinsic HR. After 24 h, mice were subjected to the same experimental protocol but received autonomic blockers in reverse order (i.e., propranolol followed by

methylatropine) in order to calculate the sympathetic effect and the intrinsic HR.

Statistical analysis

Results for all experiments are provided as means \pm SEM. In experiments where the sample size was greater than 3 and the data were normally distributed (as determined using the D'Agostino-Pearson omnibus normality test), either a Student's *t* test or a 1-way ANOVA with a Tukey *post hoc* test was used to evaluate statistical differences between experimental groups. In experiments where the data were not normally distributed or $n = 3$, either a Mann-Whitney test or a Kruskal-Wallis test with the Dunn multiple comparison test was used to determine statistical significance. All statistical analyses were performed by GraphPad Software (La Jolla, CA, USA) or SigmaStat (San Jose, CA, USA). A value of $P < 0.05$ was considered statistically significant.

Study approval

The use of human HF and control samples was approved by the institutional review board at Duke University Medical Center (Durham, NC, USA). For the animal studies, all animals were maintained and cared for according to an approved animal protocol at the University of Western Ontario (2008-127) and following Canadian Council on Animal Care guidelines.

RESULTS

VACHT levels are increased in failing human myocardium

In order to determine whether the cardiomyocyte NNCS is present in human samples, we used ventricular extracts from control individuals and patients with NICM (Table 1) and analyzed cholinergic markers. mRNA levels for AChE were not altered in HF individuals compared with non-failing controls (Fig. 1A). Similarly, mRNA levels for ChAT were slightly but not significantly ($P = 0.1511$) increased in human HF samples compared with age-matched healthy controls (Fig. 1B). Immunoblot and immunofluorescence analysis confirmed that ChAT protein levels were not altered in HF (Fig. 1C, D) and showed the presence of ChAT immunoreactivity in cardiomyocytes (Fig. 1D, arrows). The specificity of the ChAT antibody was demonstrated by the lack of protein detection in samples from conditional ChAT-KO mice.

In contrast to lack of changes in ChAT and AChE levels, VACHT mRNA levels were significantly increased in HF patients compared with age-matched controls (Fig. 1E). Immunoblot and immunofluorescence analyses indicated that VACHT protein levels were also increased in HF patients compared with controls (Fig. 1F, G). Furthermore, examination of sections costained with VACHT and α -actinin suggests that the increased levels of VACHT at least in part originated in cardiomyocytes (Fig. 1G, arrows).

cVACHT mice exhibit increased Ang II-mediated cardiac dysfunction and remodeling

In order to clarify whether changes in the expression levels of VACHT and consequently ACh secretion could affect

TABLE 1. Disease profile of patients with end-stage NICM

Patient	Diagnosis	Age (yr)
1	End-stage dilated NICM; EF 15–20%; s/p AICD; HTN	69
2	Dilated NICM; calcified aortic and mitral valves; IABP	67
3	End-stage NICM; hypertrophic dilated CM; inotrope dependent	61
4	Dilated CM; DM2; HTN; HLD	59
5	Dilated NICM; EF <15%; s/p ICD	58
6	End-stage dilated NICM; s/p AICD	56
7	End-stage NICM; some LVH; possible dilated CM <i>via</i> MR; right ventricular dysfunction; lupus	64

AICD, automatic implantable cardioverter defibrillator; CM, cardiomyopathy; DM2, diabetes mellitus type 2; EF, ejection fraction; HLD, hyperlipidemia; HTN, hypertension; IABP, intra-aortic balloon pump; ICD, implantable cardioverter defibrillator; LVH, left ventricular hypertrophy; MR, mitral regurgitation.

pathologic remodeling, we used cVACHT mice, which have decreased secretion of ACh. We treated cVACHT mice chronically with Ang II or saline. Ang II is a potent vasoconstrictor that activates AT₁ receptors on vascular smooth muscle cells (33, 34) and can thereby induce ventricular remodeling (35). Furthermore, Ang II-mediated signaling has also been shown to directly induce hypertrophy and molecular remodeling in ventricular cardiomyocytes (36–38). We chose a pharmacologic treatment instead of surgical induction of HF in mice in an attempt to produce moderate cardiac dysfunction, in the event that the lack of non-neuronal cholinergic signaling led to worse outcomes.

Ang II treatment in cVACHT mice led to a significantly greater decrease in LV fractional shortening and ejection fraction compared with control animals, as assessed through noninvasive analysis of LV hemodynamics using M-mode echocardiography (Fig. 2A–C). We observed no LV dilation after Ang II treatment in cVACHT mice, and LV internal dimensions were similar to control mice both in diastole and systole (Fig. 2D).

In order to determine pathologic hallmarks in cVACHT mice that may contribute to the worsened LV function observed after Ang II, heart weight and cardiomyocyte surface area were analyzed. VACHT^{flox/flox} control mice displayed an increase in heart weight after Ang II treatment compared with saline-treated mice (Fig. 3A). Conversely, cVACHT mice displayed baseline cardiac hypertrophy with saline treatment alone, as we previously described (21); however, compared with saline-treated animals, Ang II treatment did not induce further significant increase in heart weight in cVACHT mice (Fig. 3A). However, an analysis of cardiomyocyte surface area *in situ* revealed that Ang II-treated cVACHT mice exhibited a significantly greater cardiomyocyte hypertrophic response than Ang II-treated control mice (Fig. 3B).

Chronic Ang II exposure can lead to increased reactive oxygen species production and cardiomyocyte death (39–41). We observed that under baseline conditions with saline treatment there was an increase in oxidative stress in the hearts of cVACHT mice compared with control mice (Fig. 3C). Furthermore, Ang II treatment led to a greater

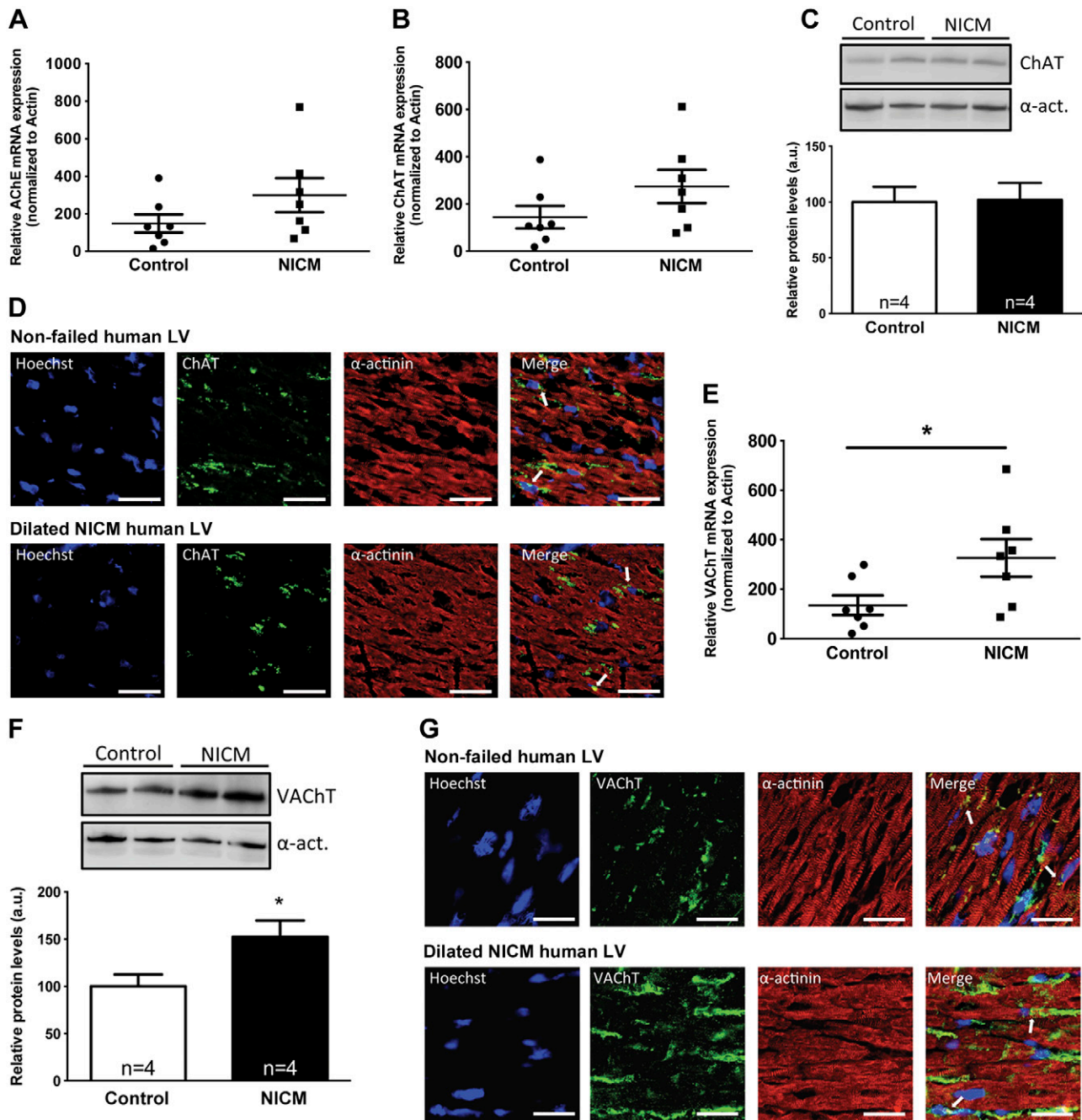


Figure 1. Human cardiomyocytes express markers of cholinergic system. *A*) mRNA levels for AChE are unaltered in NICM. *B,C*) No difference in ChAT mRNA (*B*) or protein level (*C*) is observed in NICM. *D*) Perinuclear staining for ChAT is observed in cardiomyocytes from both nonfailing and NICM samples. *E, F*) VAcHT mRNA (*E*) and protein (*F*) levels are increased in NICM. *G*) Punctate VAcHT staining is observed in perinuclear region of cardiomyocytes and increased in NICM samples. mRNA levels were analyzed by qPCR; data are presented as means \pm SEM. $n \geq 4$ subjects for all experiments. Scale bar = 25 μ m. Student's *t* test was used to determine statistical differences. * $P < 0.05$.

increase in oxidative stress in the myocardium in cVAcHT mice compared with Ang II-treated control mice (Fig. 3C).

In addition to the changes in oxidative stress, Ang II-treated cVAcHT mice displayed a greater disruption of myocardial structure compared with VAcHT^{flox/flox} control mice (Fig. 3D). An increase in fibrotic response was observed after treatment with Ang II in VAcHT^{flox/flox} and cVAcHT mice; however, in cVAcHT mice, more prominent

fibrosis due to increased interstitial and perivascular collagen deposition was observed (Fig. 3E).

cChAT mice display altered HR regulation and cardiac remodeling

VAcHT is part of the major facilitator superfamily of transporters, which includes members of the multidrug

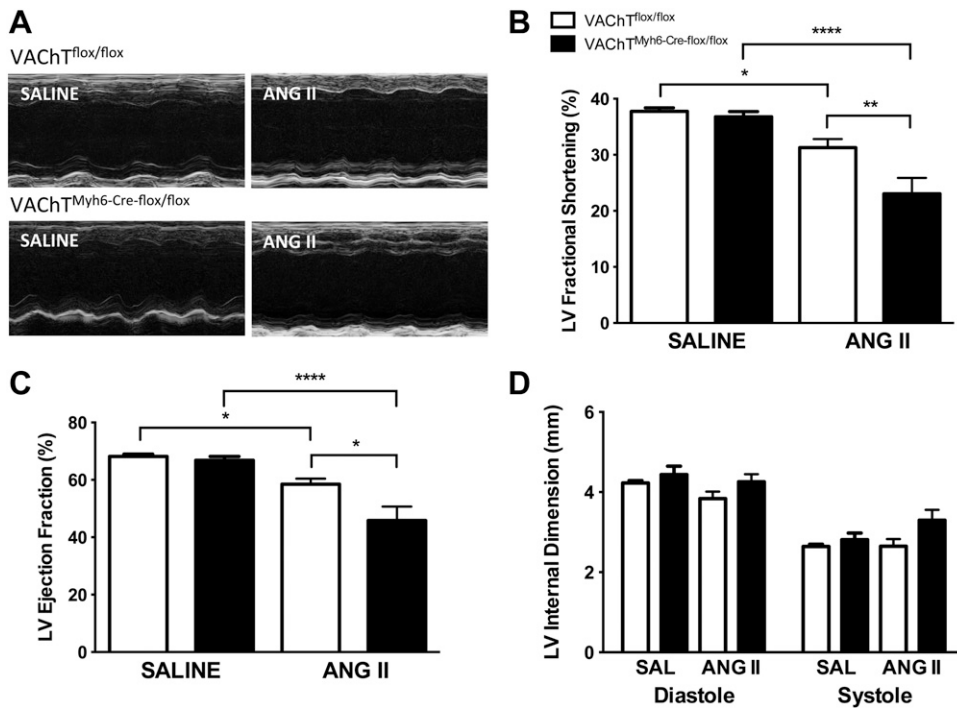


Figure 2. Cardiac dysfunction in Ang II-treated control and cVAcHT mice. *A*) Representative images of M-mode echocardiography to assess cardiac function in VAcHT^{flox/flox} control and cVAcHT mice after Ang II treatment. *B, C*) LV fractional shortening (*B*) and ejection fraction (*C*) in control and cVAcHT mice. *D*) LV internal dimensions in VAcHT^{flox/flox} mice and cVAcHT mice after Ang II treatment. Data are represented as means ± SEM. $n \geq 7$ mice for all experiments. Kruskal-Wallis test (with Dunn multiple comparison test) was used to determine statistical differences. * $P < 0.05$, ** $P < 0.01$, **** $P < 0.0001$.

resistance protein family, and has been shown to transport other organic substrates, including choline (42, 43). To provide causal relationship for a role of secreted ACh, we used mice in which cardiomyocyte-specific ACh synthesis was selectively eliminated (cChAT mice).

cChAT mice, which lack expression of ChAT in cardiomyocytes (Supplemental Fig. S1A, B), did not display changes in baseline HR (Supplemental Fig. S1C) compared with littermate controls. However, they exhibited delayed HR recovery after handling stress using an intraperitoneal injection of saline (Supplemental Fig. S1D) or after acute low-intensity treadmill exercise test (Supplemental Fig. S1E). In addition, cChAT cardiomyocytes displayed hypertrophy and molecular remodeling (Supplemental Fig. S2). These results are essentially the same as we previously reported for cVAcHT mice (21), suggesting that elimination of either ACh synthesis or its secretion from cardiomyocytes causes similar cardiovascular phenotypes.

cChAT mice exhibit enhanced Ang II-mediated cardiac dysfunction and remodeling

Similar to cVAcHT mice, Ang II treatment led to a significant decrease in LV fractional shortening and LV ejection fraction in both control and cChAT mice (Supplemental Fig. S3A–C). Interestingly, cardiac function in cChAT mice was impaired under baseline conditions. Furthermore, cChAT mice exhibited a significantly greater decrease in both LV fractional shortening and ejection fraction compared with Ang II-treated control mice (Supplemental Fig. S3B, C), thus suggesting that cChAT mice were more sensitive to Ang II-mediated cardiac dysfunction. In contrast to the experiments using cVAcHT mice, Ang II-treatment led to LV dilation in cChAT, but not control mice (ChAT^{flox/flox}; Supplemental Fig. S3D). These results

suggest that cChAT mice may have a slightly stronger phenotype than cVAcHT mice, especially considering the fact that cChAT mice show basal cardiac dysfunction, which is not as apparent in cVAcHT mice.

In contrast to Ang II-treated cChAT and cVAcHT mice, a separate set of control experiments revealed that *Myh6-Cre*⁺ mice displayed ventricular dysfunction similar to WT littermates after Ang II treatment (Supplemental Fig. S4). However, distinct from control mice, *Myh6-Cre*⁺ mice displayed enhanced ventricular dilation during systole after Ang II treatment compared with saline-treated mice (Supplemental Fig. S4D).

To further examine whether the enhanced molecular remodeling observed in cVAcHT mice was due to impaired secretion of cardiac nonneuronal acetylcholine, pathologic remodeling was also analyzed in saline- and Ang II-treated cChAT mice. ChAT^{flox/flox} mice did not display a significant increase in heart weight after Ang II treatment compared with saline-treated mice (Supplemental Fig. S5A). In contrast, cChAT mice displayed a significant increase in heart weight after Ang II treatment compared with saline-treated cChAT animals (Supplemental Fig. S5A). Although baseline characterization of cChAT mice revealed cardiac hypertrophy, this phenotype was not observed in saline-treated cChAT mice. The disparity in the observed cardiac hypertrophy might be because mice used in the present Ang II experiment were younger (3 to 4 mo) than those used for baseline measurements (Supplemental Fig. S2; 5 to 6 mo). It is possible that the hypertrophic response in cChAT mice is an age-dependent phenotype.

When compared with saline-treated ChAT^{flox/flox} animals, saline-treated cChAT mice displayed cardiomyocyte hypertrophy (Supplemental Fig. S5B). Furthermore, although both control and cChAT mice displayed a significant increase in cardiomyocyte surface area after Ang II treatment, cChAT mice exhibited significantly greater

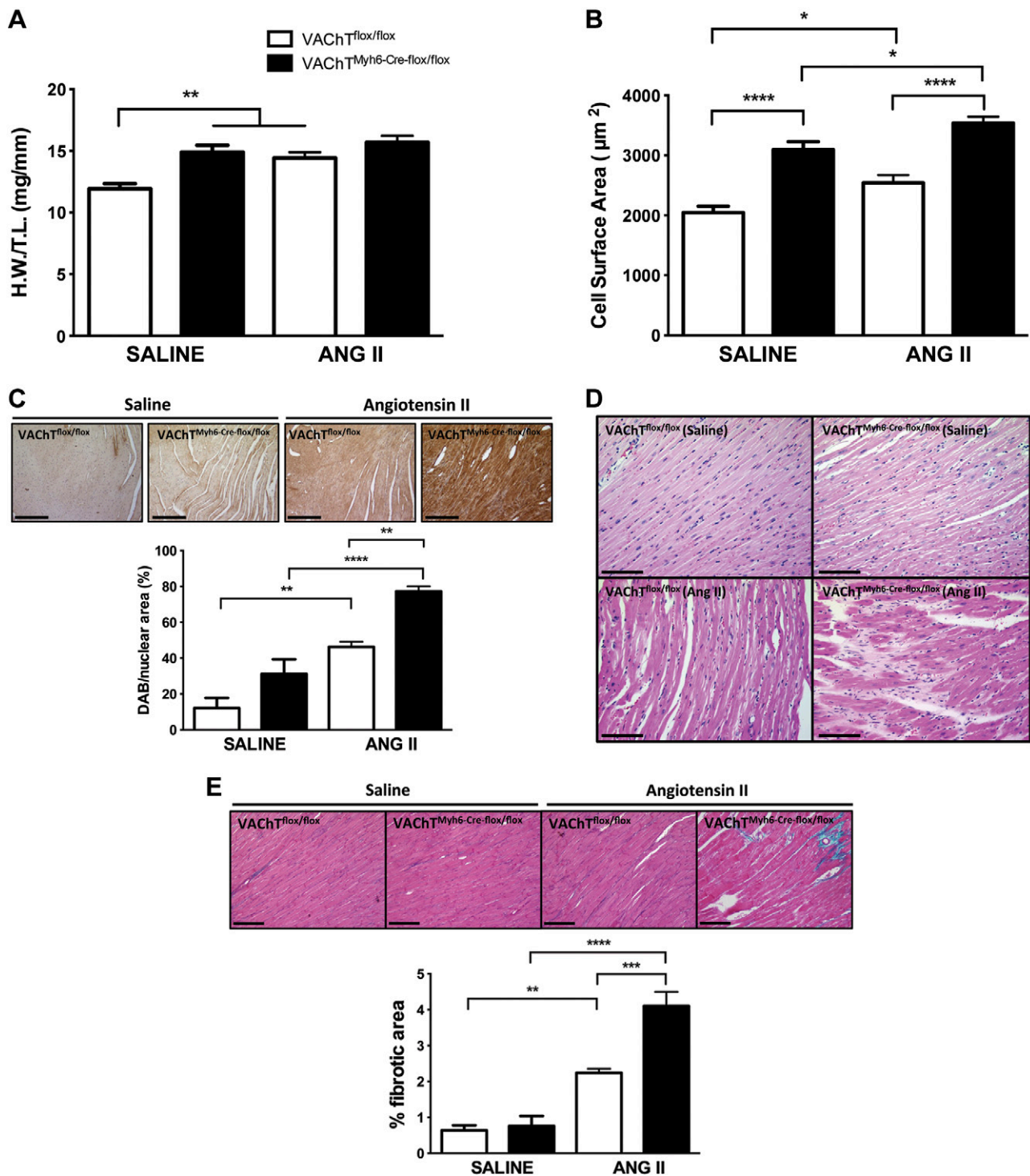


Figure 3. Ventricular hypertrophy and pathologic remodeling in VAcHT^{flox/flox} and cVAcHT mice after Ang II treatment. *A*) Heart weight/tibia length (HW/TL) ratio to assess cardiac hypertrophy. *B*) Cardiomyocyte hypertrophy after Ang II treatment in both genotypes. *C*) Analysis of myocardial oxidized protein levels in control and cVAcHT mice. *D*) Qualitative analysis of myocardial structure to determine extent of myocardial disruption and damage. *E*) Analysis of collagen deposition and fibrosis in VAcHT^{flox/flox} and cVAcHT hearts. Data are represented as means \pm SEM. $n \geq 4$ mice for all experiments. Scale bar = 60 μ m. One-way ANOVA (with Tukey multiple comparison test) was used to determine statistical differences. * $P < 0.05$, ** $P < 0.01$, *** $P < 0.001$, **** $P < 0.0001$.

myocyte hypertrophy than ChAT^{flox/flox} control mice (Supplemental Fig. S5B).

Analysis of oxidative stress in control and cChAT mice after Ang II treatment revealed similar results as those observed in Ang II-treated cVAcHT mice. cChAT mice

showed an increase in oxidized protein levels compared with ChAT^{flox/flox} controls (Supplemental Fig. S5C). Ang II treatment in both control and cChAT mice led to an increase in myocardial oxidative stress. Although cChAT mice displayed a tendency for increased levels of oxidative

stress compared with control mice, this result did not reach statistical significance ($P = 0.0726$, Supplemental Fig. S5C). Hematoxylin and eosin staining revealed that Ang II-treated cChAT mice exhibited a greater disruption of myocardial structure compared with ChAT^{flox/flox} control mice (Supplemental Fig. S5D). Additionally, trichrome C staining revealed that both ChAT^{flox/flox} and cChAT mice had significantly increased collagen deposition after Ang II treatment; however, the fibrotic response in Ang II-treated cChAT mice was significantly greater than that observed in ChAT^{flox/flox} animals (Supplemental Fig. S5E).

Analysis of pathologic damage and oxidized protein levels in Ang II-treated *Myh6-Cre*⁺ mice revealed that hearts from mice expressing Cre have similar response as WT controls (Supplemental Fig. S6). These results suggest that Cre expression at this age does not contribute to the worse remodeling observed in cChAT or vVChT mice, suggesting that paracrine/autocrine cholinergic signaling can offset pathology during remodeling.

Increased VChT expression does not disturb cardiac function

To determine whether increased levels of VChT observed in human patients would have functional consequences, we utilized mice overexpressing VChT (*ChAT-ChR2-EYFP*) for these experiments (44). This particular line was generated to express channelrhodopsin-2 (ChR2) in cholinergic neurons using a ChAT bacterial artificial chromosome (BAC); however, because the VChT gene is present in the first intron of the ChAT gene, the transgene caused VChT overexpression (27). We first confirmed whether the heart of *ChAT-ChR2-EYFP* mice overexpressed VChT. In this line, the ChR2 protein is tagged with EYFP. Immunostaining confirmed the expression of EYFP in cholinergic neurons, which were specifically labeled with the cholinergic marker CHT1 (Fig. 4A). qPCR analysis revealed that expression of the transgene in the heart led to a significant increase in VChT mRNA levels (Fig. 4B). Furthermore, immunostaining confirmed an increase in staining for VChT, thus suggesting an increase in VChT protein levels in *ChAT-ChR2-EYFP* atrial tissue (Fig. 4C). Notably, VChT levels were also up-regulated in ventricular cardiomyocytes, suggesting that the BAC transgene is also expressed in cardiomyocytes (Fig. 4D). In accordance with these data, we also observed increased secretion of ACh from isolated tissue (Fig. 4E, F).

In order to determine whether this increase in VChT levels leads to cardiovascular physiologic changes in these mice, we performed tail-cuff analysis to measure blood pressure and HR. No difference in HR or blood pressure was observed between the 2 genotypes using the CODA tail-cuff system, in which mice need to be immobilized (Fig. 5A). In contrast, the more sensitive electrocardiographic analysis revealed that baseline HR in *ChAT-ChR2-EYFP* mice over 24 h was significantly lower than control mice (Fig. 5B), with the main difference in HR being observed during the light cycle (Fig. 5C). Additionally, administration of a bolus dose of the muscarinic receptor antagonist methylatropine led to a significantly greater increase in the HR of *ChAT-ChR2-EYFP* mice compared with WT animals (Fig. 5D). Alternatively, there was no

difference in HR response between the 2 genotypes after administration of the β -adrenergic receptor antagonist propranolol (Fig. 5D). These data suggest that the hearts of *ChAT-ChR2-EYFP* mice are under greater parasympathetic control than WT animals. In fact, this notion is further supported by the fact that the initial increase in HR after an acute, low-intensity treadmill test is attenuated in *ChAT-ChR2-EYFP* mice compared with control counterparts (Fig. 5E), suggesting that response to increased physiologic stress may be offset by the augmented levels of VChT.

In order to determine whether this increase in cholinergic tone leads to changes in basal LV hemodynamics, we used the Millar catheter technique to assess cardiac function in live animals. Analysis of LV parameters in anesthetized animals was done under both baseline conditions and after the administration of isoproterenol (0.5 μ g i.p.). All of the hemodynamic parameters measured using the Millar technique were similar between WT controls and *ChAT-ChR2-EYFP* mice, both under baseline conditions and after a bolus dose of isoproterenol (Table 2). These results suggest that under baseline conditions, increased VChT expression does not alter LV function.

Ang II-mediated cardiac dysfunction and pathologic remodeling is attenuated in *ChAT-ChR2-EYFP* mice

Similar to the previous experiments with vVChT and cChAT mice, we chronically treated *ChAT-ChR2-EYFP* mice with Ang II, which led to a significant decrease in LV fractional shortening and LV ejection fraction in WT control mice (Fig. 6A–C). Conversely, Ang II-treated *ChAT-ChR2-EYFP* mice did not display a significant decrease in either LV fractional shortening or ejection fraction (Fig. 6B, C).

Analysis of pathologic remodeling after Ang II treatment revealed that WT mice display both cardiac and cardiomyocyte hypertrophy, whereas *ChAT-ChR2-EYFP* mice seemed to be protected (Fig. 7A, B). In addition, *ChAT-ChR2-EYFP* mice did not show a significant increase in oxidative stress after Ang II treatment, which could be easily detected in WT mice (Fig. 7C). In addition to attenuated oxidative stress, qualitative analysis of the myocardium revealed that disruption of myocardial structure was reduced in Ang II-treated *ChAT-ChR2-EYFP* mice compared with WT animals (Fig. 7D). Finally, the fibrotic response after Ang II treatment was only observed in WT, but not *ChAT-ChR2-EYFP*, mice (Fig. 7E).

DISCUSSION

The role of parasympathetic signaling in heart disease is still not fully understood, but autonomic imbalance with reduced parasympathetic activity has been described (8–10). Here we provide evidence that in HF VChT levels are increased in the ventricles and specifically in cardiomyocytes. This observation is in line with previous work that revealed a transdifferentiation-induced increase in the expression of cholinergic markers in HF (12). Furthermore, it was previously shown that the expression of cholinergic markers in ventricular myocytes is related to myocardial ACh availability. Increasing ACh levels using

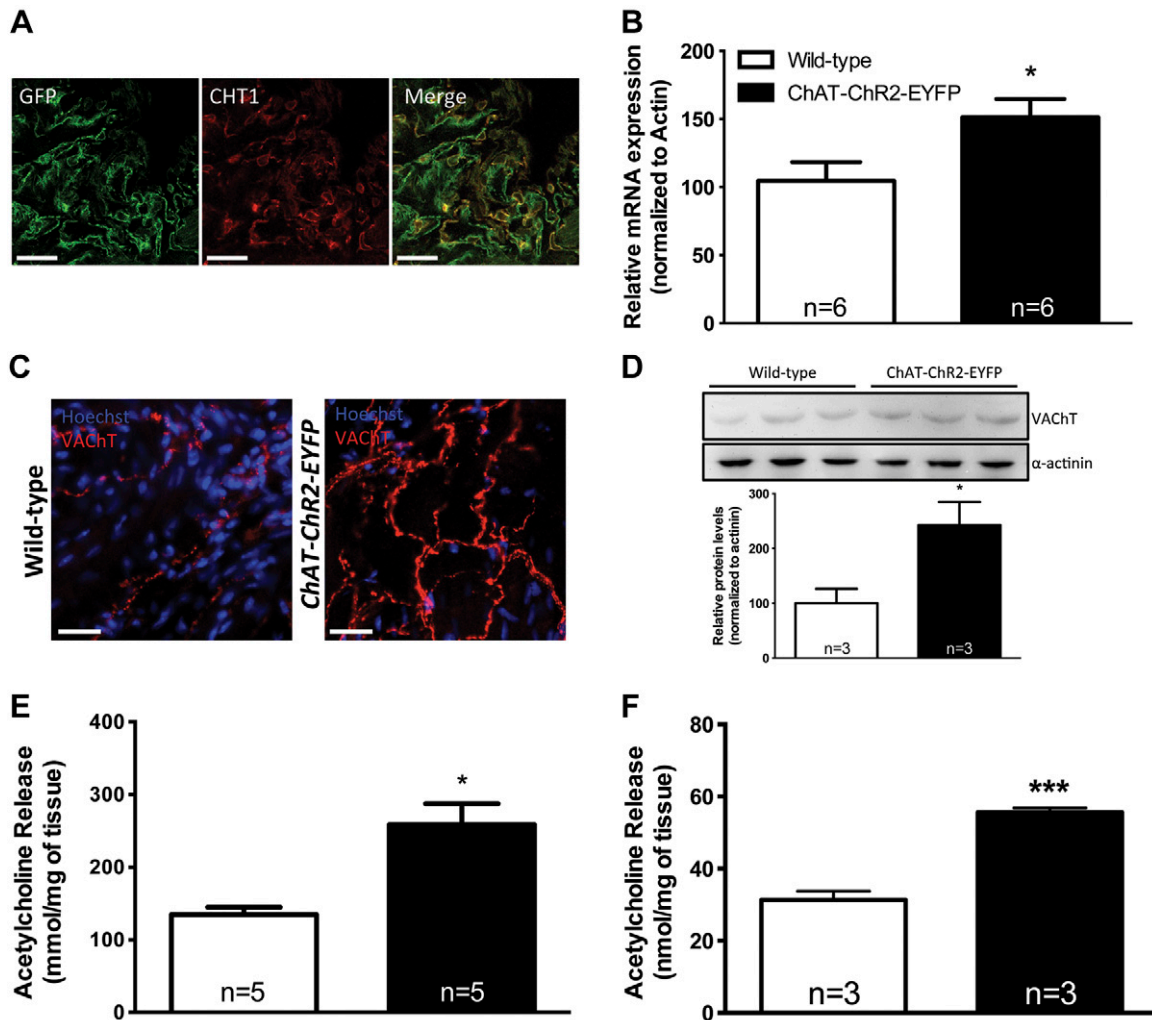


Figure 4. Characterization of VACHT expression and ACh release in *ChAT-ChR2-EYFP* hearts. A) Expression of BAC transgene containing *ChR2-EYFP* in CHT1-labeled cholinergic neurons in atria of *ChAT-ChR2-EYFP* mice. B) VACHT mRNA expression in *ChAT-ChR2-EYFP* hearts, as analyzed by qPCR. C) Immunostaining for VACHT in WT and *ChAT-ChR2-EYFP* atria. D) VACHT protein levels in ventricular cardiomyocytes isolated from WT and *ChAT-ChR2-EYFP* mice. E and F) Analysis of ACh release through HPLC with electrochemical detection (E) and colorimetric assay (F) in WT and *ChAT-ChR2-EYFP* hearts. Data are represented as means \pm SEM. n = at least 3 mice per genotype for all experiments. Scale bar = 25 μ m. Statistical differences were analyzed by Student's t test (A, E) or Mann-Whitney test (D, F). * P < 0.05, *** P < 0.001.

pyridostigmine led to a significant down-regulation of non-neuronal cholinergic machinery in cardiomyocytes (18). Conversely, the expression of ChAT and VACHT in ventricular myocytes was up-regulated after treatment with the sympathetic agonist isoproterenol. Together, these observations suggest that in response to decreased vagal activity there are multiple compensatory increases in cholinergic markers in HF.

To our knowledge, this is the first report to reveal the existence of a NNCS in human cardiomyocytes and to report augmented VACHT expression in HF. This increase in VACHT levels in human patients with NICM and HF hints at the possibility that ventricular myocytes may be able to increase cardiac ACh secretion as a compensation for decreased vagal activity.

We used mice that reproduced the increase in VACHT levels (*ChAT-ChR2-EYFP*) and determined that increased cholinergic signaling did not lead to adverse effects in the cardiovascular system. In fact, our experiments revealed

that although the increase in ACh release does not alter basal LV contractility in these mice, the hearts of *ChAT-ChR2-EYFP* mice are under greater parasympathetic control and also display an attenuated increase in exercise-induced HR. These data suggest that under physiologic conditions, enhancing cholinergic signaling plays a role in regulating chronotropic, but not inotropic, responses. The blunted response to activity further suggests that increased ACh signaling in the heart may lead to greater control of the heart under conditions of increased sympathetic drive, as seen in disease states.

The enhanced cholinergic signaling in *ChAT-ChR2-EYFP* mice also mitigated Ang II-mediated ventricular remodeling. These genetically modified mice did not develop LV dysfunction and pathological remodeling to the same extent as WT mice after challenge with Ang II. This observation is in line with previous work suggesting that increasing ACh levels yields positive results in HF (12–18). The fact that an increase in systemic ACh secretion in mice

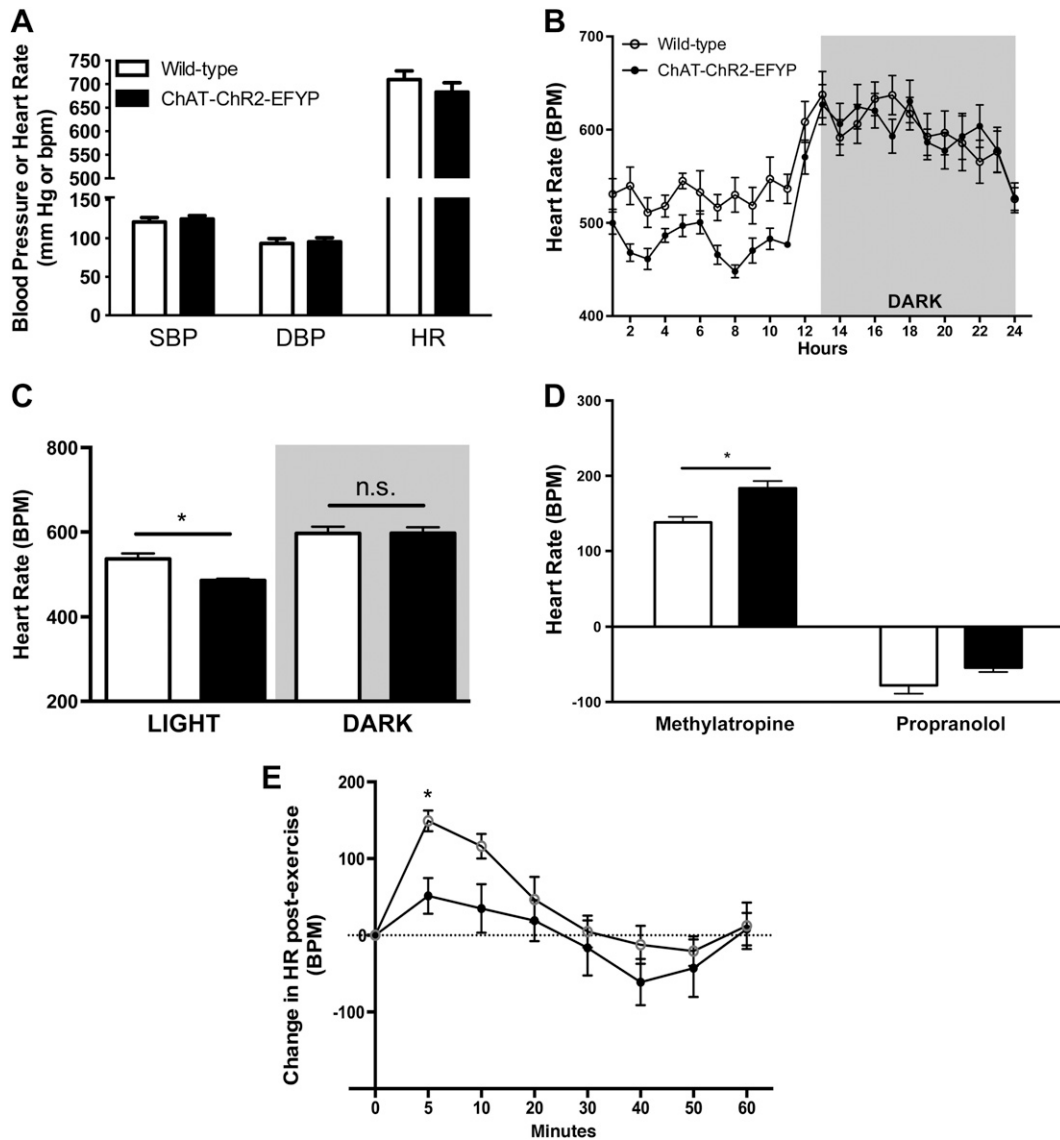


Figure 5. Parasympathetic regulation of cardiac function in *ChAT-ChR2-EYFP* mice. *A*) Systolic and diastolic blood pressure and HR using CODA tail-cuff system in WT and *ChAT-ChR2-EYFP* mice. *B*) HR over 24 h in awake, free-moving WT and *ChAT-ChR2-EYFP* mice in their home cage. *C*) Comparison of mean HR during light and dark cycles between 2 genotypes. *D*) HR response to acute bolus dose of atropine or propranolol in WT and *ChAT-ChR2-EYFP* mice. *E*) HR response to short burst of exercise in WT controls and *ChAT-ChR2-EYFP* mice. $n \geq 7$ mice for all experiments. Data are represented as means \pm SEM. Statistical differences were analyzed by either Student's *t* test (*A*, *C*, *D*) or 2-way ANOVA (with Sidak multiple comparison test) (*B*, *E*). $*P < 0.05$.

partially offsets the deleterious effects of Ang II suggests that the increase in VAcHT levels seen in failing human myocardium may help to delay progression of HF in humans.

Given that *ChAT-ChR2-EYFP* mice overexpress VAcHT in both cardiac parasympathetic neurons and ventricular cardiomyocytes, there is a possibility that some of the positive effects observed in these transgenic mice after Ang II treatment are due to increased activity of the cardiac NNCS. In order to test this possibility, we used mice lacking either the ability to produce (cChAT mice) or release (cVAcHT mice) ACh. Our results revealed that the NNCS plays a key role in regulating the extent of cardiac disease. Chronic treatment with Ang II in cChAT and cVAcHT mice led to enhanced cardiac remodeling characterized by increased oxidative stress and myocyte hypertrophy. It is

likely that the heightened disruption of myocardial structure and increased fibrotic response in KO mice contributes to the observed LV dysfunction and decreased ventricular compliance. These data suggest that the NNCS normally plays a critical role in attenuating the ventricular remodeling response.

It is possible that the increased oxidative stress observed in cChAT and cVAcHT mice leads to cardiomyocyte death, which may serve as a precursor for the accelerated ventricular remodeling and dysfunction associated with chronic Ang II infusion. The molecular mechanisms that regulate this enhanced remodeling response by secreted ACh have yet to be fully elucidated. Long-term cholinergic signaling *via* muscarinic receptors may regulate the expression of key components of cardiomyocyte stress-related proteins (45–47). Alternatively, the NNCS may

TABLE 2. Hemodynamic parameters for control ($n = 7$) and ChAT-ChR2-EYFP ($n = 7$) mice at baseline and after isoproterenol stimulation

Parameter	Baseline		Isoproterenol	
	WT	ChAT-ChR2	WT	ChAT-ChR2
HR (bpm)	324 ± 28	260 ± 16	636 ± 33	588 ± 30
LVSP (mmHg)	112.1 ± 3.3	107.3 ± 4.1	105.8 ± 9.4	105.4 ± 5.1
LVEDP (mmHg)	9.3 ± 1.7	8.0 ± 1.4	1.3 ± 1.3	0.7 ± 1.0
+dP/dT _{max} (mmHg/s)	9190 ± 509	8078 ± 383	14,940 ± 1116	16,802 ± 726
-dP/dT _{min} (mmHg/s)	-8516 ± 608	-8246 ± 491	-10,623 ± 1068	-10,231 ± 795
Contractility index (s ⁻¹)	178.3 ± 8.3	164.6 ± 1.5	329.9 ± 20.5	339.6 ± 12.3

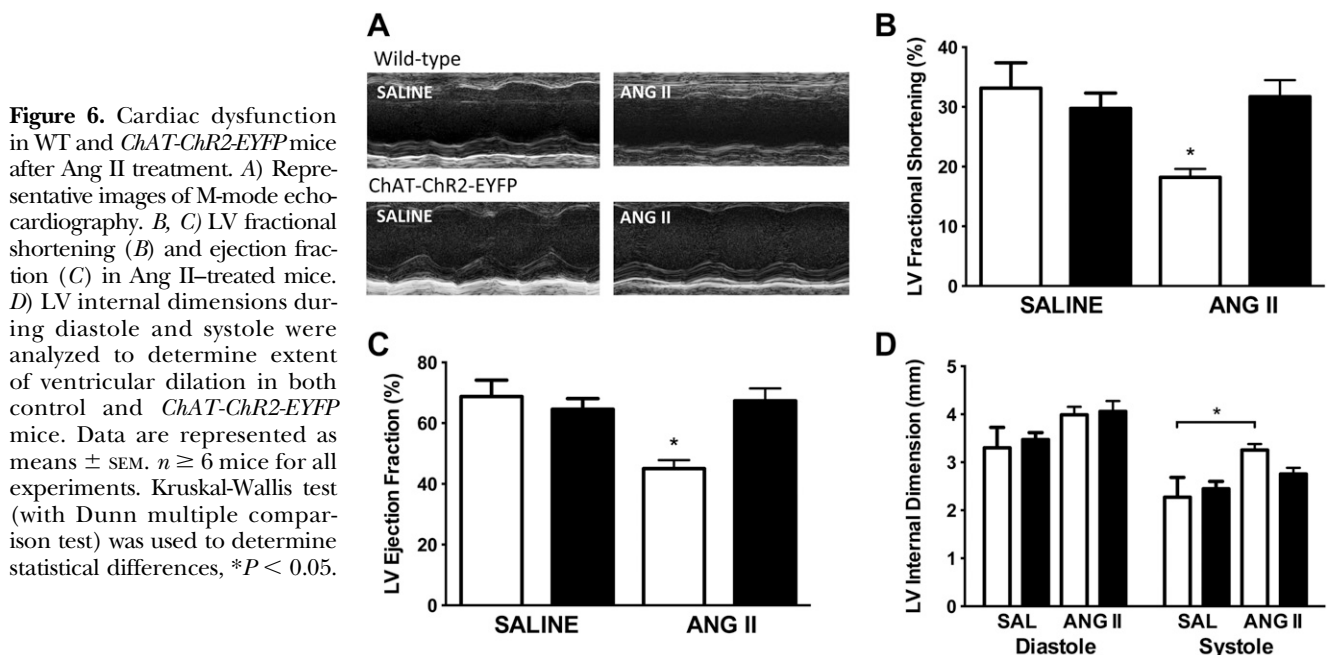
+dP/dT_{max}, maximum first derivative of change in LV pressure; -dP/dT_{min}, minimum first derivative of change in LV pressure; LVEDP, left ventricular end diastolic pressure; LVSP, left ventricular systolic pressure. Values are presented as means ± SEM.

regulate cardiomyocyte function in a non-cell-autonomous way by regulating local inflammatory responses. It is well established that cholinergic activity controls innate inflammatory responses by secretion of ACh from a subpopulation of T cells, the so-called cholinergic anti-inflammatory pathway (48–50). Whether secretion of ACh from cardiomyocytes may regulate local inflammatory cells in the heart remains to be determined. It is noteworthy, however, that inflammation contributes to cardiac remodeling and dysfunction in HF (51–56).

In agreement with the current study, previous work from other groups has also demonstrated the importance of the NNCS. Cardiomyocyte-specific overexpression of the enzyme choline acetyltransferase (ChAT-Tg) attenuates ventricular remodeling and increases survival after myocardial infarction by mechanisms regulating cellular stress (24). ChAT-KO HL-1 cells, derived from murine atrial cardiac tissue, exhibit decreased viability in response to chemical hypoxia (57). These studies further implicate the cardiac NNCS in the regulation of cardiac function, especially after induction of stress, including ischemia.

It remains to be determined whether vagal stimulation can also increase activity of the NNCS. Vagal stimulation is known to increase overall cholinergic signaling in the heart and improve cardiovascular parameters in experimental HF (13, 14), an effect that can be mimicked by using cholinesterase inhibitors (15–17). Although the mechanisms through which treatment with cholinesterase inhibitors can induce protective effects have yet to be explored, a nationwide cohort study from Sweden revealed that the use of cholinesterase inhibitors in Alzheimer disease patients leads to a 34% reduction in risk of myocardial infarction and death (20). It is possible that at least some of the positive effects observed in response to increased cholinergic activity using cholinesterase inhibitors are due to enhanced signaling of the cardiac NNCS.

We propose that the increase in VAcHT levels in HF may not be deleterious but rather may help to offset cardiac remodeling. Obviously, this increase in VAcHT expression does not completely prevent remodeling in end-stage disease, but experiments in mice suggest that ventricular remodeling in HF would be worse in the absence of this compensatory mechanism. Our data indicate



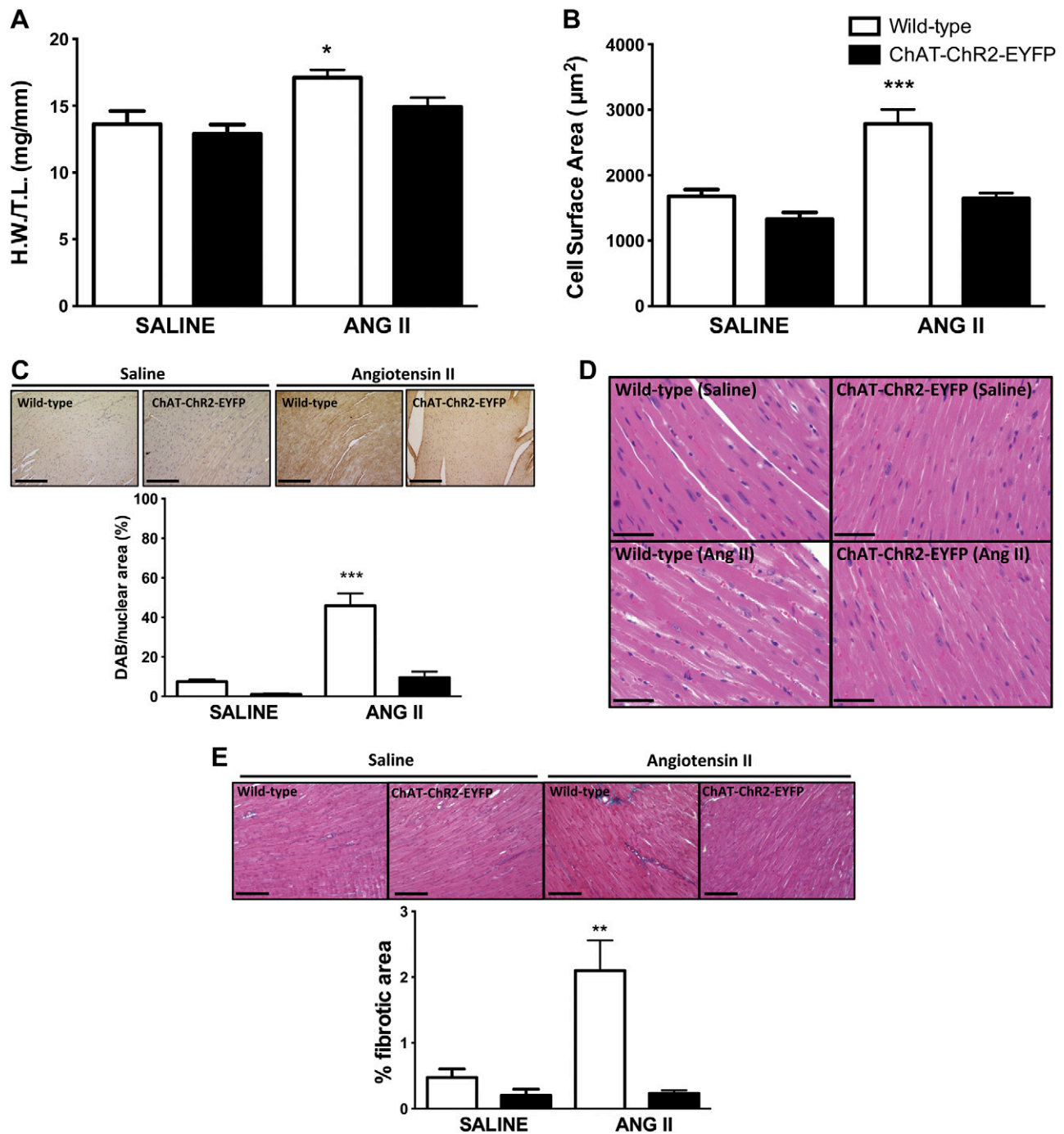


Figure 7. Ang II-mediated ventricular hypertrophy and remodeling in WT and *ChAT-ChR2-EYFP* mice. **A)** Heart weight/tibia length (HW/TL) ratio in saline and Ang II-treated WT and *ChAT-ChR2-EYFP* mice. **B)** Cardiomyocyte cell surface area in WT and *ChAT-ChR2-EYFP* mice. **C)** Levels of myocardial oxidized protein after Ang II treatment in both genotypes. **D)** Qualitative analysis of myocardial structure and disruption in both genotypes. **E)** Collagen deposition in WT and *ChAT-ChR2-EYFP* mice. Data are represented as means \pm SEM. $n \geq 4$ mice for all experiments. Scale bar = 60 μ m. One-way ANOVA (with Tukey multiple comparison test) was used to determine statistical differences. * $P < 0.05$, ** $P < 0.01$, *** $P < 0.001$.

that cardiomyocyte-secreted ACh plays a critical role in regulating the onset and progression of LV dysfunction in mice. Up-regulation of markers of the cholinergic system may partially restore cholinergic signaling to baseline levels after vagal withdrawal. In addition, increased cholinergic signaling may counteract the effects of the increased sympathetic drive observed in heart disease. Our results support the notion that increased

cholinergic signaling, such as that achieved by cholinesterase inhibitors, may lead to positive outcomes in HF patients. Cholinesterase inhibitors are well characterized as a treatment option in patients with Alzheimer disease; therefore, modulation of both neuronal parasympathetic signaling and NNCS through the use of cholinesterase inhibitors may serve as an unexplored clinical avenue for the treatment of cardiac disease in humans. **[F]**

The authors thank M. Watson (Duke Human Heart Repository) for assistance in obtaining human HF samples. This work was supported by the Heart and Stroke Foundation of Ontario (NA6656 and G-13-0002843), Canadian Institutes for Health Research (MOP-82756 and MOP-89919), Canadian Foundation for Innovation, the Ontario Research Fund, and the U.S. National Institutes for Health Fogarty International Center Grant R03TW008425 to S.G. S.G. was supported by CAPES (Coordenação de Aperfeiçoamento de Pessoal de Nível Superior), FAPEMIG (Fundação de Amparo à Pesquisa do Estado de Minas Gerais), and CNPq (Conselho Nacional de Desenvolvimento Científico e Tecnológico). H.C.S. was supported by FAPESP (Fundação de Amparo à Pesquisa do Estado de São Paulo). R.G. was supported by a New Investigator Award from the Heart and Stroke Foundation of Canada. A.R. was supported by an Ontario Graduate Scholarship. G.C.S.V.T. received a FAPESP postdoctoral fellowship.

REFERENCES

- Mann, D. L. (1999) Mechanisms and models in heart failure: a combinatorial approach. *Circulation* **100**, 999–1008
- Braunwald, E., and Bristow, M. R. (2000) Congestive heart failure: fifty years of progress. *Circulation* **102**(Suppl 4), IV14–IV23
- Floras, J. S. (2009) Sympathetic nervous system activation in human heart failure: clinical implications of an updated model. *J. Am. Coll. Cardiol.* **54**, 375–385
- Massie, B. M. (1988) Is neurohormonal activation deleterious to the long-term outcome of patients with congestive heart failure? I. Introduction. *J. Am. Coll. Cardiol.* **12**, 547–550
- Hasking, G. J., Esler, M. D., Jennings, G. L., Burton, D., Johns, J. A., and Korner, P. I. (1986) Norepinephrine spillover to plasma in patients with congestive heart failure: evidence of increased overall and cardiorenal sympathetic nervous activity. *Circulation* **73**, 615–621
- Rockman, H. A., Koch, W. J., and Lefkowitz, R. J. (2002) Seven-transmembrane-spanning receptors and heart function. *Nature* **415**, 206–212
- DiPiro, J., Talbert, R. L., Yee, G. C., Matzke, G. R., Wells, B. G., and Posey, L. M. (2008) *Pharmacotherapy: A Pathophysiological Approach*, Vol. 1. McGraw-Hill, New York
- Binkley, P. F., Nunziata, E., Haas, G. J., Nelson, S. D., and Cody, R. J. (1991) Parasympathetic withdrawal is an integral component of autonomic imbalance in congestive heart failure: demonstration in human subjects and verification in a paced canine model of ventricular failure. *J. Am. Coll. Cardiol.* **18**, 464–472
- Grassi, G., Seravalle, G., Bertinieri, G., Turri, C., Stella, M. L., Scopelliti, F., and Mancina, G. (2001) Sympathetic and reflex abnormalities in heart failure secondary to ischaemic or idiopathic dilated cardiomyopathy. *Clin. Sci.* **101**, 141–146
- Grassi, G., Seravalle, G., Cattaneo, B. M., Lanfranchi, A., Vailati, S., Giannattasio, C., Del Bo, A., Sala, C., Bolla, G. B., and Pozzi, M. (1995) Sympathetic activation and loss of reflex sympathetic control in mild congestive heart failure. *Circulation* **92**, 3206–3211
- Kinugawa, T., and Dibner-Dunlap, M. E. (1995) Altered vagal and sympathetic control of heart rate in left ventricular dysfunction and heart failure. *Am. J. Physiol.* **268**, R310–R316
- Kanazawa, H., Ieda, M., Kimura, K., Arai, T., Kawaguchi-Manabe, H., Matsuhashi, T., Endo, J., Sano, M., Kawakami, T., Kimura, T., Monkawa, T., Hayashi, M., Iwanami, A., Okano, H., Okada, Y., Ishibashi-Ueda, H., Ogawa, S., and Fukuda, K. (2010) Heart failure causes cholinergic transdifferentiation of cardiac sympathetic nerves via gp130-signaling cytokines in rodents. *J. Clin. Invest.* **120**, 408–421
- Li, M., Zheng, C., Sato, T., Kawada, T., Sugimachi, M., and Sunagawa, K. (2004) Vagal nerve stimulation markedly improves long-term survival after chronic heart failure in rats. *Circulation* **109**, 120–124
- Zhang, Y., Popovic, Z. B., Bibevski, S., Fakhry, I., Sica, D. A., Van Wagoner, D. R., and Mazgalev, T. N. (2009) Chronic vagus nerve stimulation improves autonomic control and attenuates systemic inflammation and heart failure progression in a canine high-rate pacing model. *Circ Heart Fail* **2**, 692–699
- Handa, T., Katare, R. G., Kakinuma, Y., Arikawa, M., Ando, M., Sasaguri, S., Yamasaki, F., and Sato, T. (2009) Anti-Alzheimer's drug, donepezil, markedly improves long-term survival after chronic heart failure in mice. *J. Card. Fail.* **15**, 805–811
- Li, M., Zheng, C., Kawada, T., Inagaki, M., Uemura, K., Shishido, T., and Sugimachi, M. (2013) Donepezil markedly improves long-term survival in rats with chronic heart failure after extensive myocardial infarction. *Circ. J.* **77**, 2519–2525
- Lataro, R. M., Silva, C. A., Fazan, R., Jr., Rossi, M. A., Prado, C. M., Godinho, R. O., and Salgado, H. C. (2013) Increase in parasympathetic tone by pyridostigmine prevents ventricular dysfunction during the onset of heart failure. *Am. J. Physiol. Regul. Integr. Comp. Physiol.* **305**, R908–R916
- Gavioli, M., Lara, A., Almeida, P. W., Lima, A. M., Damasceno, D. D., Rocha-Resende, C., Ladeira, M., Resende, R. R., Martinelli, P. M., Melo, M. B., Brum, P. C., Fontes, M. A., Souza Santos, R. A., Prado, M. A., and Guatimosim, S. (2014) Cholinergic signaling exerts protective effects in models of sympathetic hyperactivity-induced cardiac dysfunction. *PLoS One* **9**, e100179
- Schwartz, P. J., De Ferrari, G. M., Sanzo, A., Landolina, M., Rordorf, R., Raineri, C., Campana, C., Revera, M., Ajmone-Marsan, N., Tavazzi, L., and Odero, A. (2008) Long term vagal stimulation in patients with advanced heart failure: first experience in man. *Eur. J. Heart Fail.* **10**, 884–891
- Nordström, P., Religa, D., Wimo, A., Winblad, B., and Eriksdotter, M. (2013) The use of cholinesterase inhibitors and the risk of myocardial infarction and death: a nationwide cohort study in subjects with Alzheimer's disease. *Eur. Heart J.* **34**, 2585–2591
- Roy, A., Fields, W. C., Rocha-Resende, C., Resende, R. R., Guatimosim, S., Prado, V. F., Gros, R., and Prado, M. A. (2013) Cardiomyocyte-secreted acetylcholine is required for maintenance of homeostasis in the heart. *FASEB J.* **27**, 5072–5082
- Roy, A., Lara, A., Guimarães, D., Pires, R., Gomes, E. R., Carter, D. E., Gomez, M. V., Guatimosim, S., Prado, V. F., Prado, M. A., and Gros, R. (2012) An analysis of the myocardial transcriptome in a mouse model of cardiac dysfunction with decreased cholinergic neurotransmission. *PLoS One* **7**, e39997
- Lara, A., Damasceno, D. D., Pires, R., Gros, R., Gomes, E. R., Gavioli, M., Lima, R. F., Guimarães, D., Lima, P., Bueno, C. R., Jr., Vasconcelos, A., Roman-Campos, D., Menezes, C. A., Sirvente, R. A., Salemi, V. M., Mady, C., Caron, M. G., Ferreira, A. J., Brum, P. C., Resende, R. R., Cruz, J. S., Gomez, M. V., Prado, V. F., de Almeida, A. P., Prado, M. A., and Guatimosim, S. (2010) Dysautonomia due to reduced cholinergic neurotransmission causes cardiac remodeling and heart failure. *Mol. Cell. Biol.* **30**, 1746–1756
- Kakinuma, Y., Tsuda, M., Okazaki, K., Akiyama, T., Arikawa, M., Noguchi, T., and Sato, T. (2013) Heart-specific overexpression of choline acetyltransferase gene protects murine heart against ischemia through hypoxia-inducible factor-1 α -related defense mechanisms. *J. Am. Heart Assoc.* **2**, e004887
- Kent, K. M., Epstein, S. E., Cooper, T., and Jacobowitz, D. M. (1974) Cholinergic innervation of the canine and human ventricular conducting system. Anatomic and electrophysiologic correlations. *Circulation* **50**, 948–955
- Roy, A., Guatimosim, S., Prado, V. F., Gros, R., and Prado, M. A. (2014) Cholinergic activity as a new target in diseases of the heart. *Mol. Med.* **20**, 527–537
- Kolisnyk, B., Guzman, M. S., Raulic, S., Fan, J., Magalhães, A. C., Feng, G., Gros, R., Prado, V. F., and Prado, M. A. (2013) *ChAT-ChR2-EYFP* mice have enhanced motor endurance but show deficits in attention and several additional cognitive domains. *J. Neurosci.* **33**, 10427–10438
- Crittenden, J. R., Lacey, C. J., Lee, T., Bowden, H. A., and Graybiel, A. M. (2014) Severe drug-induced repetitive behaviors and striatal overexpression of VACHT in *ChAT-ChR2-EYFP* transgenic mice. *Front. Neural Circuits* **8**, 57
- Zhao, S., Ting, J. T., Atallah, H. E., Qiu, L., Tan, J., Gloss, B., Augustine, G. J., Deisseroth, K., Luo, M., Graybiel, A. M., and Feng, G. (2011) Cell type-specific channelrhodopsin-2 transgenic mice for optogenetic dissection of neural circuitry function. *Nat. Methods* **8**, 745–752
- Rocha-Resende, C., Roy, A., Resende, R., Ladeira, M. S., Lara, A., de Moraes Gomes, E. R., Prado, V. F., Gros, R., Guatimosim, C., Prado, M. A., and Guatimosim, S. (2012) Non-neuronal cholinergic machinery present in cardiomyocytes offsets hypertrophic signals. *J. Mol. Cell. Cardiol.* **53**, 206–216
- Lau, J. K., Brown, K. C., Thornhill, B. A., Crabtree, C. M., Dom, A. M., Witte, T. R., Hardman, W. E., McNees, C. A., Stover, C. A., Carpenter, A. B., Luo, H., Chen, Y. C., Shiflett, B. S., and Dasgupta, P. (2013) Inhibition of cholinergic signaling causes apoptosis in human bronchioalveolar carcinoma. *Cancer Res.* **73**, 1328–1339

32. Beraldo, F. H., Soares, I. N., Goncalves, D. F., Fan, J., Thomas, A. A., Santos, T. G., Mohammad, A. H., Roffé, M., Calder, M. D., Nikolova, S., Hajj, G. N., Guimaraes, A. L., Massensini, A. R., Welch, L., Betts, D. H., Gros, R., Drangova, M., Watson, A. J., Bartha, R., Prado, V. F., Martins, V. R., and Prado, M. A. (2013) Stress-inducible phosphoprotein 1 has unique cochaperone activity during development and regulates cellular response to ischemia *via* the prion protein. *FASEB J.* **27**, 3594–3607
33. Sugaya, T., Nishimatsu, S., Tanimoto, K., Takimoto, E., Yamagishi, T., Imamura, K., Goto, S., Imaizumi, K., Hisada, Y., Otsuka, A., Uchida, H., Sugiura, M., Fukuta, K., Fukamizu, A., and Murakami, K. (1995) Angiotensin II type 1a receptor-deficient mice with hypotension and hyperreninemia. *J. Biol. Chem.* **270**, 18719–18722
34. Oliverio, M. I., Best, C. F., Kim, H. S., Arendshorst, W. J., Smithies, O., and Coffman, T. M. (1997) Angiotensin II responses in AT1A receptor-deficient mice: a role for AT1B receptors in blood pressure regulation. *Am. J. Physiol.* **272**, F515–F520
35. Marano, G., Formigari, R., and Vergari, A. (1997) Effects of angiotensin II on myocardial contractility during short-term pressor responses to angiotensin II. *J. Hypertens.* **15**, 1019–1025
36. Sadoshima, J., and Izumo, S. (1993) Molecular characterization of angiotensin II-induced hypertrophy of cardiac myocytes and hyperplasia of cardiac fibroblasts. Critical role of the AT1 receptor subtype. *Circ. Res.* **73**, 413–423
37. Sadoshima, J., Xu, Y., Slayter, H. S., and Izumo, S. (1993) Autocrine release of angiotensin II mediates stretch-induced hypertrophy of cardiac myocytes *in vitro*. *Cell* **75**, 977–984
38. Shanmugam, P., Valente, A. J., Prabhu, S. D., Venkatesan, B., Yoshida, T., Delafontaine, P., and Chandrasekar, B. (2011) Angiotensin-II type 1 receptor and NOX2 mediate TCF/LEF and CREB dependent WISP1 induction and cardiomyocyte hypertrophy. *J. Mol. Cell. Cardiol.* **50**, 928–938
39. Goldenberg, I., Grossman, E., Jacobson, K. A., Shneyvays, V., and Shainberg, A. (2001) Angiotensin II-induced apoptosis in rat cardiomyocyte culture: a possible role of AT1 and AT2 receptors. *J. Hypertens.* **19**, 1681–1689
40. Laursen, J. B., Rajagopalan, S., Galis, Z., Tarpey, M., Freeman, B. A., and Harrison, D. G. (1997) Role of superoxide in angiotensin II-induced but not catecholamine-induced hypertension. *Circulation* **95**, 588–593
41. Nishiyama, A., Fukui, T., Fujisawa, Y., Rahman, M., Tian, R. X., Kimura, S., and Abe, Y. (2001) Systemic and regional hemodynamic responses to tempol in angiotensin II-infused hypertensive rats. *Hypertension* **37**, 77–83
42. Bravo, D. T., Kolmakova, N. G., and Parsons, S. M. (2004) Choline is transported by vesicular acetylcholine transporter. *J. Neurochem.* **91**, 766–768
43. Bravo, D. T., Kolmakova, N. G., and Parsons, S. M. (2005) New transport assay demonstrates vesicular acetylcholine transporter has many alternative substrates. *Neurochem. Int.* **47**, 243–247
44. Ren, J., Qin, C., Hu, F., Tan, J., Qiu, L., Zhao, S., Feng, G., and Luo, M. (2011) Habenula “cholinergic” neurons co-release glutamate and acetylcholine and activate postsynaptic neurons *via* distinct transmission modes. *Neuron* **69**, 445–452
45. Coso, O. A., Teramoto, H., Simonds, W. F., and Gutkind, J. S. (1996) Signaling from G protein-coupled receptors to c-Jun kinase involves beta gamma subunits of heterotrimeric G proteins acting on a Ras and Rac1-dependent pathway. *J. Biol. Chem.* **271**, 3963–3966
46. Gutkind, J. S., Crespo, P., Xu, N., Teramoto, H., and Coso, O. A. (1997) The pathway connecting m2 receptors to the nucleus involves small GTP-binding proteins acting on divergent MAP kinase cascades. *Life Sci.* **60**, 999–1006
47. Coso, O. A., Chiariello, M., Yu, J. C., Teramoto, H., Crespo, P., Xu, N., Miki, T., and Gutkind, J. S. (1995) The small GTP-binding proteins Rac1 and Cdc42 regulate the activity of the JNK/SAPK signaling pathway. *Cell* **81**, 1137–1146
48. Fujii, T., Tsuchiya, T., Yamada, S., Fujimoto, K., Suzuki, T., Kasahara, T., and Kawashima, K. (1996) Localization and synthesis of acetylcholine in human leukemic T cell lines. *J. Neurosci. Res.* **44**, 66–72
49. Rinner, I., and Schauenstein, K. (1993) Detection of choline-acetyltransferase activity in lymphocytes. *J. Neurosci. Res.* **35**, 188–191
50. Pavlov, V. A., Wang, H., Czura, C. J., Friedman, S. G., and Tracey, K. J. (2003) The cholinergic anti-inflammatory pathway: a missing link in neuroimmunomodulation. *Mol. Med.* **9**, 125–134
51. Westermann, D., Lindner, D., Kasner, M., Zietsch, C., Savvatis, K., Escher, F., von Schlippenbach, J., Skurk, C., Steendijk, P., Riad, A., Poller, W., Schultheiss, H. P., and Tschöpe, C. (2011) Cardiac inflammation contributes to changes in the extracellular matrix in patients with heart failure and normal ejection fraction. *Circ. Heart Fail.* **4**, 44–52
52. Kleinbongard, P., Schulz, R., and Heusch, G. (2011) TNF α in myocardial ischemia/reperfusion, remodeling and heart failure. *Heart Fail. Rev.* **16**, 49–69
53. Mann, D. L. (2015) Innate immunity and the failing heart: the cytokine hypothesis revisited. *Circ. Res.* **116**, 1254–1268
54. Marti, C. N., Khan, H., Mann, D. L., Georgiopoulou, V. V., Bibbins-Domingo, K., Harris, T., Koster, A., Newman, A., Kritchevsky, S. B., Kalogeropoulos, A. P., and Butler, J.; Health ABC Study. (2014) Soluble tumor necrosis factor receptors and heart failure risk in older adults: Health, Aging, and Body Composition (Health ABC) Study. *Circ. Heart Fail.* **7**, 5–11
55. Lavine, K. J., Epelman, S., Uchida, K., Weber, K. J., Nichols, C. G., Schilling, J. D., Ornitz, D. M., Randolph, G. J., and Mann, D. L. (2014) Distinct macrophage lineages contribute to disparate patterns of cardiac recovery and remodeling in the neonatal and adult heart. *Proc. Natl. Acad. Sci. USA* **111**, 16029–16034
56. Epelman, S., Liu, P. P., and Mann, D. L. (2015) Role of innate and adaptive immune mechanisms in cardiac injury and repair. *Nat. Rev. Immunol.* **15**, 117–129
57. Kakinuma, Y., Akiyama, T., Okazaki, K., Arikawa, M., Noguchi, T., and Sato, T. (2012) A non-neuronal cardiac cholinergic system plays a protective role in myocardium salvage during ischemic insults. *PLoS One* **7**, e50761

Received for publication June 16, 2015.
Accepted for publication September 28, 2015.